

The Labusch parameter of a driven flux line lattice in $\text{YBa}_2\text{Cu}_3\text{O}_7$ superconducting films

A.V. Pan and P. Esquinazi^a

Department of Superconductivity and Magnetism, Institut für Experimentelle Physik II, Universität Leipzig, Linnéstrasse 5, 04103 Leipzig, Germany

Received 21 December 1999

Abstract. We have investigated the influence of a driving force on the elastic coupling (Labusch parameter) of the field-cooled state of the flux line lattice (FLL) in 400 nm thick $\text{YBa}_2\text{Cu}_3\text{O}_7$ superconducting films. We found that the FLL of a field-cooled state without driving forces is not in an equilibrium state. Results obtained for magnetic fields applied at 0° and 30° relative to CuO_2 planes, show an enhancement of the elastic coupling of the films at driving current densities several orders of magnitude smaller than the critical one. Our results indicate that the FLL appears to be in a relatively ordered, metastable state after field cooling without driving forces.

PACS. 74.76.Bz High- T_c films – 74.60.Ge Flux pinning, flux creep, and flux-line lattice dynamics

1 Introduction

The investigation of effects directly related to true phase transitions of the flux line lattice (FLL) in high-temperature superconductors (HTS) is a current topic of research. These studies are not only difficult to perform experimentally due to the necessary resolution but also their interpretation is sometimes not straightforward due to pinning effects. In the quasi-three-dimensional (3D) HTS $\text{YBa}_2\text{Cu}_3\text{O}_7$ (Y123) an anomalous enhancement of the pinning force appears to be associated with the “peak effect” (PE) in the dc critical current measured using the voltage criterion [1]. In contrast to conventional low- T_c superconductors, this PE occurs at fields much below the upper critical field, near the thermally activated depinning line [2]. Within the classical argument of Pippard [3] the PE in a 3D superconductor with a high density of pinning centers occurs if at high enough fields or temperatures the shear modulus or rigidity of the FLL strongly drops. This softening of the FLL observed with increasing temperature and/or magnetic field should overwhelm the usual decrease of the pinning force in order to have an effective enhancement of the pinning force. Within this picture the correlation between the PE and a reduction of the rigidity of the FLL is appealing.

The experimental evidence for a correlation between the PE and the “melting” of the FLL is, however, far from being clear. As noted in reference [4] the sharp *enhancement* of resistance with temperature in Y123 crystals, interpreted as a first-order melting transition [5], is precisely opposed to the enhancement of pinning expected within

Pippard’s picture. The results of a remarkable experimental study characterising the PE in a clean and anisotropic superconductor suggested that much of the transport data interpreted as melting in HTS may be related to nonequilibrium dynamical steady states of the FLL and not to true phase transitions [4].

Studies of the PE and its dependence on the magnetic field history in Y123 thin films and crystals using the vibrating reed technique [2] casted some doubts on the interpretation of the PE line as a melting line. It was suggested that the onset of the PE is due to the thermal creation of FLL dislocations and that some of the melting lines may be observations of the PE using different criteria [2]. The strongly nonlinear response of vibrating superconductors near the PE [2] is qualitatively consistent with the dynamic phase diagram measured in [4].

New features recently found in Y123 crystals by transport experiments reveal a PE at high fields in the vortex solid region of the phase diagram [6]. This PE joins smoothly the – believed to be – first-order melting line at high temperatures [6] and suggests a correlation with the previously observed PE at low fields [1,2]. The weak temperature dependence of this new PE at high fields was speculated to be the analog of the second magnetization peak observed in $\text{Bi}_2\text{Sr}_2\text{CaCu}_2\text{O}_8$ (Bi2212) HTS [6]. Recently published measurements on Y123 crystals up to 27 T reveal that the temperature dependence of the field at the second magnetization peak is qualitatively similar to that observed in Bi2212 crystals [7]. Depending on the crystal properties, the second magnetization peak can be observed even in the same temperature range, *i.e.* at $T < 50$ K, as in Bi2212 HTS [8]. Recent experimental studies cast strong doubts about the interpretation

^a e-mail: esquin@physik.uni-leipzig.de

of the second magnetization peak in Bi2212 HTS based on a pinning enhancement and related to a phase transition of the FLL [9,10]. The origin of the so-called “pre-melting” peaks in the critical current density obtained by transport measurements is therefore still unclear [6].

As the vibrating reed results in Y123 crystals and thin films showed, the observed PE depends on the magnetic history of the sample as well as on the driving force [2] provided by the reed amplitude, which in general is ≤ 150 nm. The observed history effect means that the magnitude of the PE depends whether the sample was cooled in or without a field. We note that the driving forces in a typical vibrating reed experiment are extremely low – shielding currents lower than 10^3 A/m² – which is an advantage in comparison to other methods used to study pinning properties. Therefore, it could be shown that at low enough vibrating amplitudes (low driving force) the PE vanishes in a Y123 film when measured as a function of temperature at constant field [2]. A strong driving current dependence of the PE has been also observed in 2H-NbSe₂ crystal [4]. In this crystal the dissipation near the upper critical field strongly increases with the transport current, in agreement with the observed behavior in [2], although the PE still remains [4].

Current driven order, disorder and depinning of the FLL in 2H-NbSe₂ crystals have been studied in detail in references [11–13]. The influence of the probing current on the first-order transition has been studied in Y123 crystals [14]. In contrast to those studies, the technique used in this work allows us to study the change of pinning using probing and driving currents substantially smaller than the critical one. The vibrating reed measurements provide the space derivative of the pinning force at small distances of the potential minimum. As we will show below, at low temperatures the measurements as a function of a driving dc current reveal an irreversible enhancement of the pinning of the FLL. Loading a vibrating superconductor with a transport current allows us to resolve very small changes in the elastic coupling as a function of applied current far below the vortex depinning transition $T < T_D(B_a)$ and applied forces much less than the critical ones (B_a refers to the applied magnetic field). In this paper we show that a metastable state with a distinctly higher level of pinning than that one obtained after field cooling procedure without a driving force can be reached by applying a sufficiently large driving current. Our work shows that the field-cooled state is not a state of minimum potential energy for the FLL, at least for Y123 HTS, and therefore different metastable states may be obtained depending on the used experimental procedure to study pinning-related properties.

2 Experimental details

The measuring setup is schematically depicted in Figure 1. The samples (films with substrate) were glued onto a silicon single crystal host reed. The dimensions of the host reed used in this study were (length \times width \times thickness) $l \times w \times d = 5 \times 1 \times 0.1$ mm³. The reed was

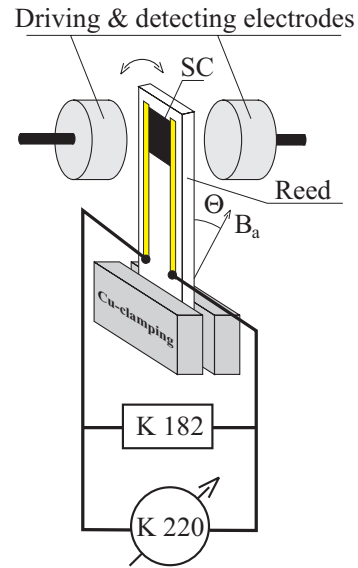


Fig. 1. Setup of the vibrating reed technique with the superconducting film (SC). The film has two electrodes for electrical contacts used for injecting the transport current along the sample width and perpendicular to the applied magnetic field direction B_a . The dc current is supplied by a Keithley 220 source (K220). The voltage drop over the sample is registered by a Keithley 182 voltmeter (K182).

T-shaped and its back-side was covered with 15 nm gold layer for the capacitive detection of the reed motion. The reed driving force supplied by a sinusoidal voltage was kept constant throughout the measurements. Detailed description of the vibrating reed technique and the typical electronic arrangement are published elsewhere [15,16]. Our system allows us to measure automatically the resonance frequency $\nu = \omega/2\pi$ of the reed as a function of field, temperature or driving current density J_T .

The YBa₂Cu₃O₇ films were produced by pulsed laser deposition technique with a rotating substrate [17]. The results presented in this work were obtained with a film of dimensions: $d_p \simeq 400$ nm, $w_p \simeq 1.2$ mm, and $l_p \simeq 1.6$ mm. The film was deposited on a thin (0.1 mm) SrTiO₃ substrate to minimize the total sample weight glued to the host reed. The characterization of the film has been done with resistivity, $I - V$ characteristics, critical current and depinning line measurements and reported in reference [18]. The normal state resistivity of the film just above the superconducting transition was $\rho_n \sim 30\mu\Omega$ cm and its critical temperature $T_c = 89$ K with a transition width ~ 0.5 K. The critical current density defined at 2 μ V follows $J_c(T) = J_c(0)(1 - (T/T_c))^{1.88}$ with $J_c(0) \simeq 1.5 \times 10^{11}$ A/m² at $B_a = 2$ T.

The virgin field-cooled state was achieved by cooling down in a magnetic field through the superconducting transition temperature to the temperature of the measurements without applying a current load. The maximum current load applied in the measurements was 100 mA. The measurements have been performed with the field applied parallel to the CuO₂ planes of the film ($\theta = 0^\circ \pm 1^\circ$)

and at $\theta = 30^\circ$. No differences between the results obtained for the two different angles were observed.

3 Flux line tension and elastic pinning correction in vibrating superconductors

The resonance frequency enhancement of a vibrating superconductor as a function of applied magnetic field B_a is due to the restoring force as a result of a pinned FLL. This behavior is well understood and can be quantitatively accounted for by the theory developed in [19] (for a review see Refs [15,16]). We would like to outline here the main results of the theory and restrict ourselves to the configuration depicted in Figure 1 having the sample glued on a host reed and the magnetic field applied parallel (or slightly tilted) to the length of the host reed and to the ab -planes of the films.

A superconducting sample with pinned FLL vibrating in a magnetic field distorts the field around the superconductor and consequently a positive restoring force increases the resonance frequency of the cantilever. In this case, for a sample with dimension $l_p \geq w_p \gg d_p$ the magnetic line tension can be approximated by

$$P \simeq \frac{\pi w_p}{4d_p} w_p d_p \frac{B_a^2 l_p}{\mu_0 l}. \quad (1)$$

The condition of large enough pinning is satisfied for

$$l_p \gg \Lambda_{44}, \quad (2)$$

where $\Lambda_{44} = \lambda_{44}(\pi w_p/4d_p)^{1/2}$ is the effective Campbell penetration depth for tilt waves and $\lambda_{44} = (c_{44}/\alpha)^{1/2}$ with $c_{44} = B_a^2/\mu_0$ the FLL tilt modulus. The Labusch parameter or elastic coupling between FLL and the superconducting matrix is

$$\alpha(B_a, T) = \frac{\partial^2}{\partial s^2} U(s, B_a, T)|_{s \rightarrow 0} = \left| \frac{F_p}{s_p} \right|, \quad (3)$$

where U is the mean value of the interaction energy per unit length (or pinning potential) between vortices and pinning centers, $F_p = B_a J_c$ is the volume pinning force, s is the flux line displacement relative to the superconducting matrix, s_p is the characteristic range of the pinning potential and J_c the critical current density.

The field dependence of the resonance frequency depends on the ratio of the magnetic $W_M \simeq Pl$ to mechanical $W_R \simeq I\omega^2(0)$ energies and the pinning strength of the FLL. For $X = 1.33(Pl/I\omega^2(0)) < 1$ and if (2) holds, the ideal enhancement (infinite pinning case) of the resonance frequency is given by [16]

$$\omega_i^2(B_a) - \omega^2(0) \simeq Pl/I, \quad (4)$$

where I is the inertia moment of the cantilever with sample. This is obtained experimentally at low enough temperatures and applied fields where equation (4) holds. In

the present work we determined $I \simeq 5.8 \times 10^{-11} \text{ kg m}^2$ for the used cantilever.

The field dependence of the resonance frequency is in general influenced by the finite pinning which is taken into account by a correction term ω_{pin}^2 . Non-local and end effects due to the finite length of the sample are also taken into account through the correction terms ω_{nl}^2 and ω_{end}^2 , along with a correction term due to the finite damping of the reed Γ^2 . The field dependence of the resonance frequency can be then approximated by [19]

$$\omega^2(B_a) - \omega^2(0) \simeq \frac{Pl}{I} - \omega_{\text{pin}}^2 - \omega_{\text{nl}}^2 - \omega_{\text{end}}^2 - \Gamma^2. \quad (5)$$

In general, for the geometry of the used samples $\omega_{\text{pin}}^2 \gg \omega_{\text{nl}}^2, \omega_{\text{end}}^2, \Gamma^2$.

The correction term due to the finite pinning is given by [19]

$$\omega_{\text{pin}}^2 \simeq 0.16\omega^2(0)X\tau \left(\frac{\Lambda_{44}}{l_p} \right)^2 \times \left(\frac{F(X')}{1+r/2} + \frac{p l_p G(X)}{w_p + p \Lambda_{44} \tau^{1/2}} \right), \quad (6)$$

where $F(X)$ and $G(X)$ are tabulated numerical functions [19], $X' = X/(1+4\beta X)$ with $\beta \simeq w_p^2/2\pi^2 l_p^2$; $p \simeq 0.54 \ln(0.71 w_p/d_p)$, $r = (2X)^{1/2} \Lambda_{44} \tau^{1/2}/l_p$, and $\tau \simeq 1.08$ for the case of not too strong pinning, when compressional waves penetrate the superconductor entirely ($\Lambda_{44} > d_p$).

The deviation of the measured resonance frequency from the infinite pinning value ω_i^2 is inversely proportional to α via $\omega_{\text{pin}}^2 \propto \Lambda_{44}^2 \propto \alpha^{-1}$ and therefore it allows us to numerically calculate the Labusch parameter as a function of B_a . We should note, however, that equation (6) is only an approximation for the finite pinning correction and it does not provide the correct value of α for too large ($\Lambda < d_p$) or too weak ($\omega_{\text{pin}}^2 \geq 0.1Pl/I$) pinning.

In the temperature region of interest $90 \text{ K} \geq T > 50 \text{ K}$ the Labusch parameter increases approximately as B_a^2 having a value $\alpha(B_a = 1 \text{ T}, T = 73 \text{ K}) \simeq 4 \times 10^{17} \text{ N/m}^4$ in good agreement with that obtained in reference [16] for $\text{YBa}_2\text{Cu}_3\text{O}_7$ films.

4 Results and discussion

Figure 2 shows the resonance frequency change $\nu(I_T) - \nu(0)$ as a function of the applied driven current I_T at constant field and temperature. The sample was cooled through the superconducting transition to 70 K in a field of 5 T applied parallel to the CuO_2 planes. The current dependence of the virgin state is given by the solid symbols in Figure 2. We clearly observe that the resonance frequency increases with applied current indicating, as explained in the last section, an increase of the elastic constant. The resonance frequency reaches a maximum at a current $I_0 \sim 10^{-2} \text{ A}$ which corresponds to $\sim 10^{-4} J_c(70 \text{ K}, 5 \text{ T})$. At larger currents the resonance frequency slightly decreases. Decreasing the current, the resonance frequency

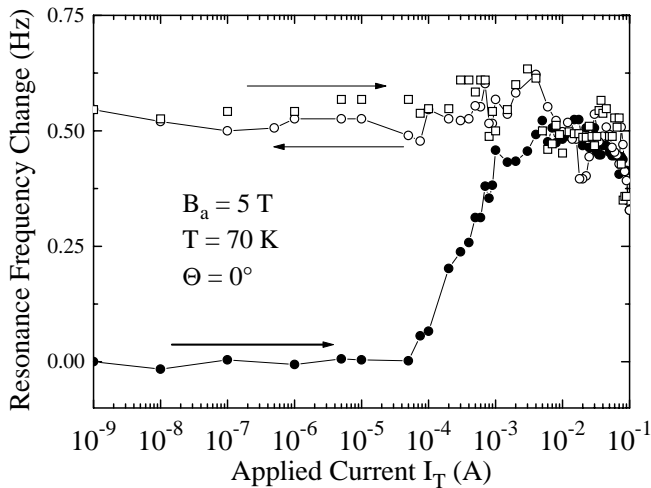


Fig. 2. The resonance frequency change as a function of the applied transport current at $T = 70$ K, applied field $B_a = 5$ T parallel to the sample main surface ($\theta = 0^\circ$). Solid symbols were obtained from the virgin FC state increasing the current; the points with open symbols were obtained by decreasing and increasing again the applied current.

follows the virgin curve down to the current where the resonance frequency shows the maximum. For lower currents the resonance frequency remains practically current independent. This irreversible behavior is observed in the temperature ($60 \text{ K} < T < 75 \text{ K}$) and field range ($B_a \leq 5 \text{ T}$) when the resonance frequency increases with current in the field-cooled virgin state.

Figure 3 shows the normalized elastic coupling as a function of the applied current density at two applied fields and at different constant temperatures, calculated from the measured resonance frequency change using equations (5, 6). All curves were measured starting from the field-cooled and zero-current virgin state. Different behavior is observed at different temperatures of the measurement. At low enough temperatures (*e.g.* $T < 60$ K) α remains independent of the applied current up to high current densities (a slight decrease of α is observed at the highest currents). The current independence of α at low T is interpreted as due to the relatively large pinning which is not overwhelmed in the available applied current density range.

Increasing temperature (*e.g.* $T > 60$ K), a maximum in α as a function of applied current clearly develops, see Figure 3. The increase in α reaches a maximum at a certain temperature (*e.g.*, at $T \simeq 70$ K at $B_a = 1$ T). For higher temperatures, eventually α decreases with applied current and shows no clear maximum within experimental resolution. In general, we can assume that the observed temperature dependence of $\alpha(I_T)$ results from the competing influence of pinning and shear modulus $c_{66}(B_a, T)$ of the FLL at low temperatures and thermally activated flux flow at high temperatures. We note that the absence of a “peak effect” in α as a function of current at high enough temperatures does not imply the absence of the

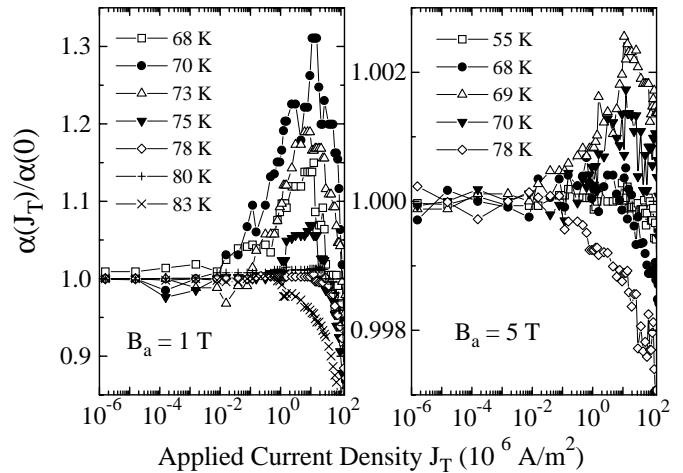


Fig. 3. Current dependence of the normalized Labusch parameter measured at two different fields at different temperatures. Lines are only a guide to the eye.

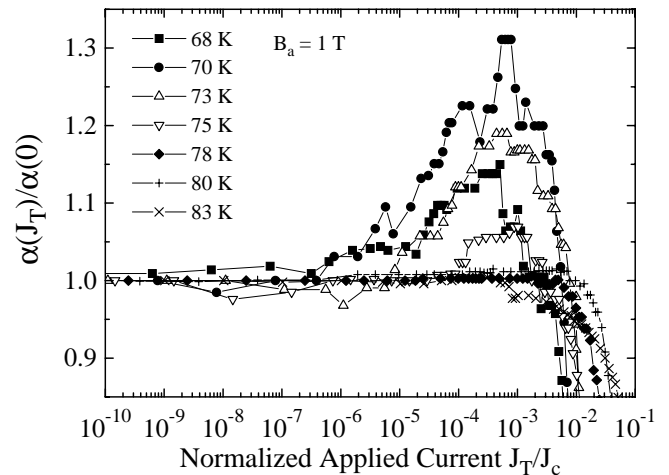


Fig. 4. Normalized Labusch parameter as a function of normalized current density at $B_a = 1$ T and at different temperatures. J_c is the critical current density.

commonly observed “peak effect” in α as a function of temperature at a constant driving force.

Figure 4 shows the normalized elastic constant as a function of the normalized applied current for a field of 1 T at different temperatures. This behavior is similar to that observed for other fields, see Figure 3. It is interesting to note that the peak in α is reached at a current of the order of 10^{-3} of the critical current density. The critical current density is obtained from the $I - V$ characteristic curves and defined at the voltage $V = 2\mu\text{V}$. We note that the rearrangement of the FLL is clearly observed already at currents several orders of magnitude smaller. We would like also to stress that the changes in α are observed at a field (or temperature) much below the corresponding depinning line $B_a \simeq 470[\text{T}](1-t)^{1.4}$ with $t = T_D(B_a)/T_D(0)$ measured at $I_T = 0$, $T_D(0) = 88$ K [18]. The shift of the depinning line with transport current is less than 2 K at the maximum applied current of 100 mA and at fields $B_a \leq 5$ T [18].

The maximum increase in α with driving current observed in our samples is of the order of 30%, see Figure 4, in the measured field range ($B_a \geq 1$ T). This increase agrees with the low-limit increase of pinning for defective FLL obtained by computer simulation studies [20]. The FLL defects produced by the driving current are probably dislocations. These are also created by thermal disorder and may lead to an enhancement in the pinning strength when measured as a function of temperature.

The results clearly indicate that the field cooled FLL is in a metastable, relatively ordered state. Upon field cooling the superconducting sample through the superconducting and (thermally activated) depinning transitions, the flux lines have to accommodate themselves in usually a random pinning centers matrix taking into account the balance between two contributions: vortex-vortex and vortex-pinning centers interactions. For our case of strong applied fields $B_a \gg B_{c1}$ we can assume that the vortex-vortex interaction overwhelms the pinning contribution at temperatures above and just below the depinning line. If the driving currents used to measure the pinning properties are small enough in order not to perturbate the FLL, regions of the FLL remain frozen in a metastable state. The observation of a peak effect will depend therefore on the magnetic history and the perturbation amplitude used to detect the pinning strength. The clear amplitude – or driving force – and magnetic history dependence of the peak effect observed near the depinning transition in reference [2] points out the importance of defects in the FLL to produce the peak effect. The driving current applied at constant field and temperature causes the arrangement of the FLL into a more disordered state and the elastic coupling increases. For intermediate fields, we expect that the higher the applied field the smaller will be the increase of α produced by the driving current since the vortex-vortex interaction increases whereas the current driven production of the defects in the FLL weakens. This behavior is observed experimentally, see Figure 3. After reaching a maximum coupling at a current I_0 , the decrease of the resonance frequency can be understood as due to the decrease of the current dependent pinning barrier. This pinning barrier is field and temperature dependent and, therefore, the observed decrease in α depends also on these parameters.

Our results are in good agreement with the conclusions obtained by transport and decoration experiments in 2H-NbSe₂ crystals [21]. In this work [21] the authors found that the number of defects in the vortex structure increases when the FLL starts to depin. The FLL becomes nearly defect-free for large enough applied currents because the vortex-vortex interaction overwhelms. Our results show, see Figure 4, that at large driven currents $J_T > 10^{-2} J_c$ the elastic coupling decreases and therefore the pinning. At high enough driven currents we expect a depinned and obviously more ordered FLL than any lattice in the FC state without driving forces.

At this point we would like to compare the published data on the peak effect measured with the vibrating reed technique in Y123 films and crystals [2] as well as the

peak effect and current driven (re)organization of the FLL observed in 2H-NbSe₂ crystals [11–13]. Vibrating-reed results in Y123 thin films showed that the enhancement of α as a function of temperature at constant applied field and in the field-cooled (FC) state is observed only if the driving force (or vibrating amplitude of the superconducting sample) is large enough. In contrast to the FC state, the zero-field cooled (ZFC) state shows a weak or no signature of a pinning enhancement near the depinning line.

If the peak effect in α is observed near the depinning temperature $T_D(B_a)$, the results indicate that α in the ZFC state and near $T_D(B_a)$ is smaller than α in the FC state [2]. This observation agrees qualitatively with the smaller critical current density measured in the ZFC state in 2H-NbSe₂ at temperatures below the peak effect [12,13]. From this observation, the authors in references [12,13] proposed that the ZFC state has a more ordered FLL than the FC state, arguing that in the I_c measurements in the ZFC state the vortices enter the sample with large velocities which lead to a more ordered FLL state. We note, however, that in the case of the vibrating reed, the perturbation to the FLL is kept much smaller than that used for I_c measurements. Therefore, we think that, in general, the ZFC state has a less homogeneous field distribution in the sample than in the FC state. Increasing temperature, an effective smaller $\alpha(B_a, T)$ is measured in the ZFC state because: (a) the effective field in the sample is smaller and (b) there is a change of the effective pinning potential due to the field gradient. The differences between the ZFC and FC states vanish as soon as the thermal creation of FLL defects and the flux creep compensate the inhomogeneous field distribution.

5 Conclusion

We have shown that the field-cooled state in YBa₂Cu₃O₇ superconducting films can be driven to a lower potential equilibrium state at fields and temperatures far below the depinning transition. This new equilibrium state of the FLL has a larger elastic coupling. Our results indicate that after field cooling without driving forces, the static FLL is in a metastable, relatively *ordered* state. Its pinning can be enhanced by the current driven creation of defects in the FLL. Our results support the recently published interpretation on the “melting” transition that argues that the FLL does not melt at the depinning line but the opposite, it decouples from the superconducting matrix becoming more ordered [22]. This ordering is partially retained in the FLL after FC through the depinning line without driving forces.

We would like to acknowledge M. Lorenz for providing us with the YBa₂Cu₃O₇ superconducting films and Y. Kopelevich for a careful reading of the manuscript and fruitful discussions. This work is supported by the Deutsche Forschungsgemeinschaft within the “Innovationskolleg Phänomene an der Miniaturisierungsgrenze” (Project H, DFG IK 24/B1-1) and the German-Israeli Foundation for Scientific Research and Development (Grant G-0553-191.14/97).

References

1. W.K. Kwok, J.A. Fendrich, C.J. van der Beek, G.W. Crabtree, Phys. Rev. Lett. **73**, 2614 (1994).
2. M. Ziese, P. Esquinazi, A. Gupta, H.F. Braun, Phys. Rev. B **50**, 9491 (1994).
3. A.B. Pippard, Philos. Mag. **19**, 217 (1969).
4. M.J. Higgins, S. Bhattacharya, Physica C **257**, 232 (1996).
5. H. Safar, P.L. Gammel, D.A. Huse, D.J. Bishop, J.P. Rice, D.M. Ginsberg., Phys. Rev. Lett. **69**, 824 (1992).
6. G.W. Crabtree, W.K. Kwok, U. Welp, D. Lopez, J.A. Fendrich, in *Physics and Materials Science of Vortex States, Flux Pinning and Dynamics*, NATO Science Series, Vol. 356, edited by R. Kossowsky, S. Bose, V. Pan, Z. Durusoy (Kluwer A.P. Dordrecht, Boston, London, 1999), p. 357.
7. T. Nishizaki, T. Naito, N. Kobayashi, Physica C **282-287**, 2117 (1997), Phys. Rev. B **58**, 11169 (1998).
8. T. Nishizaki, K. Shibata, T. Naito, M. Maki, N. Kobayashi, *Proceedings of the International Conference on Physics and Chemistry of Molecular and Oxide Superconductors, Stockholm, Sweden July 1999*, to be published.
9. Y. Kopelevich, P. Esquinazi, J. Low Temp. Phys. **113**, 1 (1998).
10. Y. Kopelevich, S. Moehlecke, J.H.S. Torres, R. Ricardo da Silva, P. Esquinazi, J. Low Temp. Phys. **116**, 261 (1999).
11. W. Henderson, E.Y. Andrei, M.J. Higgins, S. Bhattacharya, Phys. Rev. Lett. **77**, 2077 (1996).
12. Z.L. Xiao, E.Y. Andrei, M.J. Higgins, Phys. Rev. Lett. **83**, 1664 (1999).
13. E.Y. Andrei, Z.L. Xiao, W. Henderson, M.J. Higgins, P. Shuk, M. Greenblatt, J. Phys. IV France **9**, Pr 10-5 (1999).
14. S.N. Gordeev, D. Bracanovic, A.P. Rassau, P.A.J. de Groot, R. Cagnon, L. Taillefer, Phys. Rev. B **57**, 645 (1998).
15. P. Esquinazi, J. Low Temp. Phys. **85**, 139 (1991).
16. M. Ziese, P. Esquinazi, H.F. Braun, Superconducting Science and Technology **7**, 869 (1994).
17. M. Lorenz, H. Hochmuth, D. Natusch, H. Börner, G. Lippold, K. Kreher, W. Schmitz, Appl. Phys. Lett. **68**, 3332 (1996).
18. A.V. Pan, F. Ciovacco, P. Esquinazi, M. Lorenz, Phys. Rev. B **60**, 4293 (1999).
19. E.H. Brandt, P. Esquinazi, H. Neckel, J. Low Temp. Phys. **63**, 187 (1986).
20. E.H. Brandt, Phys. Rev. Lett. **50**, 1599 (1983).
21. A. Duarte *et al.*, Phys. Rev. B **53**, 11336 (1996).
22. Y. Kopelevich, P. Esquinazi, Solid State Commun. **114**, 241 (2000).